A Low-Affinity Ca^{2+}-Dependent Association of Calmodulin With the Rab3A Effector Domain Inversely Correlates With Insulin Exocytosis

Hiroshi Kajio,[1] Scott Olszewski,[1] Philip J. Rosner,[2] Matthew J. Donelan,[1] Kieran F. Geoghegan,[2] and Christopher J. Rhodes[1]

The stimulus-response coupling pathway for glucose-regulated insulin secretion has implicated a rise in cytosolic $[Ca^{2+}]_i$ as a key factor to induce insulin exocytosis. However, it is unclear how elevated $[Ca^{2+}]_i$ communicates with the pancreatic β-cell's exocytotic apparatus. As Rab3A is a model protein involved in regulated exocytosis, we have focused on its role in regulating insulin exocytosis. By using a photoactivatable cross-linking synthetic peptide that mimics the effector domain of Rab3A and microsequence analysis, we found calmodulin to be a major Rab3A target effector protein in pancreatic β-cells. Coimmunoprecipitation analysis from pancreatic islets confirmed a Rab3A-calmodulin interaction in vivo, and that it inversely correlated with insulin exocytosis. Calmodulin affected neither GTPase nor guanine nucleotide exchange activity of Rab3A. The calmodulin-Rab3A interaction was pH- and Ca^{2+}-dependent, and it was preferential for GTP-bound Rab3A. However, Rab3A affinity for calmodulin was relatively low (K_d = 18–22 μmol/l at 10^{-5} mol/l $[Ca^{2+}]$) and competed by other calmodulin-binding proteins that had higher affinity (e.g., Ca^{2+}/calmodulin-dependent protein kinase-2 [CaMK-2] {K_d = 300–400 nmol/l at 10^{-5} mol/l $[Ca^{2+}]$}). Moreover, the Ca^{2+} dependence of the calmodulin-Rab3A interaction ($K_{0.5}$ = 15–18 μmol/l $[Ca^{2+}]$, maximal at 100 μmol/l $[Ca^{2+}]$) was significantly lower compared with that of the calmodulin–CaMK-2 association ($K_{0.5}$ = 40 μmol/l $[Ca^{2+}]$, maximal at 1 mmol/l $[Ca^{2+}]$). The data suggested that a transient Rab3A-calmodulin interaction might represent a means of directing calmodulin to the cytoplasmic face of a β-granule, where it can be subsequently transferred for activation of other β-granule–associated calmodulin-binding proteins as local $[Ca^{2+}]_i$ rises to promote insulin exocytosis. *Diabetes* 50: 2029–2039, 2001

From the [1]Pacific Northwest Research Institute and Department of Pharmacology, University of Washington, Seattle, Washington; and the [2]Central Research Division, Pfizer, Groton, Connecticut.

Address correspondence and reprint requests to Christopher J. Rhodes, PhD, Pacific Northwest Research Institute, 720 Broadway, Seattle, WA 98122. E-mail: cjr@pnri.org.

Received for publication 19 January 2001 and accepted in revised form 15 June 2001.

Bpa, benzoylphenylalanine; BSA, bovine serum albumin; CaM, calmodulin; CaMK-2, Ca^{2+}/calmodulin-dependent protein kinase-2; DEAE, diethylaminoethyl; GAP, GTPase-activating protein; GDI, GDP-dissociation inhibitor; GEF, guanine nucleotide exchange factor; GTP-γ-S, guanosine 5′-3-*O*-(thio) triphosphate; HPLC, high-performance liquid chromatography; Rab3A-WT, wild-type recombinant Rab3A protein; REEP, Rab3A exocytotic effector protein; RIM, Rab3-interacting molecule.

Insulin secretion from the pancreatic β-cell is regulated by certain nutrients, hormones, and pharmaceutical agents, but the most physiologically relevant stimulus of these is glucose (1,2). Increased glucose metabolism in the β-cell generates certain metabolic coupling signals (e.g., an increase in the ATP-to-ADP ratio), leading to a series of ion channel events resulting in a rise in the cytosolic $[Ca^{2+}]_i$ (1,2). It is a rise in cytosolic $[Ca^{2+}]_i$ that has long been proposed to be the key signal by which β-cell exocytosis is induced (1). However, the means by which $[Ca^{2+}]_i$ coerces β-granule transport from an intracellular storage pool toward the β-cell's surface, to be docked at a pre-exocytotic site against the plasma membrane, and then to promote secretory granule membrane/plasma membrane fusion for the final exocytotic event, is poorly understood. Moreover, it has become clear that additional regulatory factors (including certain protein kinase activities, GTP, and elevated cytosolic fatty acyl moieties [1,2]), other than a rise in $[Ca^{2+}]_i$, are necessary to instigate glucose-regulated insulin exocytosis (3,4). For the moment, it has been presumed that the molecular machinery required for insulin exocytosis in pancreatic islet β-cells will require components similar to that for synaptic vesicle exocytosis in neurons, including cofactors such as Ca^{2+} and GTP (4–6). However, despite these similarities, there are differences in the mechanism that induces a rapid triggering of synaptic vesicle exocytosis in neurons versus a relatively slower exocytosis of larger dense-core secretory granules in endocrine cells (4,7).

To gain a better insight into the molecular mechanism of regulated insulin exocytosis, we examined the role of Rab3A in β-cells. Members of the Rab class of GTP-binding proteins participate in directing vesicular transport in eukaryotic cells (8), and Rab3A is specifically involved in the mechanism of regulated exocytosis in neuroendocrine cells (6,9). When Rab3A is in an "active" GTP-bound state, it inhibits Ca^{2+} and agonist-induced hormone release from endocrine cells, suggesting that the activation or triggering of regulated exocytosis requires a downstream step in which the inhibitory action of Rab3A is overcome (10). Consequently, it has been suggested that Rab3A functions upstream of secretory granule docking and the final membrane fusion event (6,9), yet this is apparently downstream of a Ca^{2+}-requiring step in the exocytotic mechanism (11). It has been postulated that Rab3A plays its regulatory role

in the exocytotic mechanism via specific interaction with a putative effector protein, analogous to the Ras-Raf interaction (12). Indeed, Rab3A associates with at least two classes of proteins, concerned either with the guanine nucleotide–binding state of Rab3A (such as GTPase-activating protein [GAP], guanine nucleotide exchange factor [GEF] or MSS4, and GDP-dissociation inhibitor [GDI]) or proteins proposed to interact with Rab3A in the regulated exocytotic mechanism (such as rabphilin3A, rabin3, Rab3-interacting molecule [RIM], and calmodulin [13–15]). The so-called effector domain of Rab3a, analogous to the equivalent domain in Ras, is appropriately exposed on the outside of the Rab3A molecule and has been demonstrated to structurally interact with rabphilin3A (16,17). Synthetic peptides that mimic the effector domain of Rab3A induce regulated exocytosis in neuroendocrine cells (12), including pancreatic β-cells (18,19), which has supported the concept of the Rab3A effector domain interacting with a specific "effector protein" (12). However, it is unclear whether the various Rab3A effector proteins interact with different motifs on the Rab3A molecule or compete for the same Rab3A domain. We have previously used a radiolabeled and photoactivatable cross-linking Rab3A effector domain peptide ([^{125}I]Rab3AL-X) to show that the Rab3A effector domain specifically associates with a 17/20-kDa protein doublet in pancreatic β-cells. We tentatively named this doublet Rab3A exocytotic effector protein (REEP)-1 and -2 (18), but in the current study, we identify these as rat calmodulin. Calmodulin appears to be the major Rab3A-associating protein in pancreatic β-cells (14), and characterization of the biochemistry of this protein-protein interaction reveals some novel insight into the mechanism of insulin exocytosis.

RESEARCH DESIGN AND METHODS

Materials. Na[^{125}I]I and guanosine 5′-3-*O*-(thio) triphosphate (GTP-γ-[^{35}S]) were from Amersham, and [^{3}H]GDP and [γ-^{32}P]GTP were from NEN DuPont. [^{125}I]insulin was a gift from Eli Lilly. The *t*-butoxycarbonyl benzyl–protected amino acids for peptide synthesis were from Applied Biosystems, except *t*-butoxycarbonyl benzoylphenylalanine (Bpa), which was purchased from Bachem. Nycodenz was from Nycomed Pharma (Oslo, Norway), and Percoll was from Pharmacia Biotech. Biotinylated and nonbiotinylated bovine calmodulin were from Calbiochem, and magnetic Streptavidin beads were from Promega. Rab3A antisera were from Santa Cruz Biotechnology, or, as previously described for immunoprecipitation experiments (18), calmodulin and Ca^{2+}/calmodulin-dependent protein kinase-2 (CaMK-2) antisera were from Upstate Biotechnology, and MSS4 antisera were from Dr. P. De Camilli, Yale University (New Haven, CT). An immunoblot chemiluminescence detection kit was from NEN Life Sciences (Boston, MA). Unless otherwise stated, all other chemicals were purchased from Sigma or Fisher and were of the highest grade/purity available.

Tissue. Transplantable rat insulinoma tissue (20) was propagated in NEDH rats in accordance with the National Institutes of Health's guidelines for the care and use of laboratory animals. Insulinoma tissues represented an abundant source of pancreatic β-cell tissue (20). Insulinoma subcellular fractions highly enriched in insulin secretory granules, plasma membrane, and cytosol were prepared by differential, Nycodenz discontinuous density gradient, and Percoll continuous density centrifugations as described (21). Marker enzyme analysis was by insulin radioimmunoassay for secretory granules, lactate dehydrogenase was used for cytosol, and 5′-nucleotidase was used for plasma membrane (21).

Rat pancreatic islets were isolated by collagenase digestion followed by Histopaque-Ficoll density gradient centrifugation as described (22). Batches of 100 islets were preincubated for 60 min at 37°C in 300 μl Krebs-Ringer bicarbonate buffer containing 0.1% (wt/vol) bovine serum albumin (BSA), 20 mmol/l HEPES (pH 7.4), and a basal 2.8 mmol/l glucose, followed by a second 60-min incubation at 37°C at either basal 2.8 mmol/l glucose or stimulatory 16.7 mmol/l glucose. In certain experiments, 125 μmol/l oleate complexed with 0.1% (wt/vol) BSA, as described, was also added in 300 μl of the same buffer. After the second incubation, the medium was collected and analyzed for insulin secretion by radioimmunoassay. The remaining islets were washed and then placed in 300 μl lysis buffer (50 mmol/l HEPES [pH 8.0], 1% [vol/vol] Triton X-100, 100 μmol/l phenylmethylsulfonyl fluoride, 10 μmol/l *trans*-epoxysuccinyl-L-leucylamido-[4-guandino] butane, 10 μmol/l pepstatin-A, 10 μmol/l tosylphenylalanyl chloromethyl ketone, and 100 μmol/l leupeptin) and disrupted by sonication (25 W, 10 s). A 5-μl aliquot of the islet lysate was removed for analysis of islet insulin content by radioimmunoassay, whereas the remainder was subjected to immunoprecipitation as described (22).

Peptide synthesis and photoactivated peptide cross-linking. Peptide synthesis was performed as described (18), with all synthetic peptides purified by high-performance liquid chromatography (HPLC) and amino acid sequence analyses checked to be as predicted. The following peptides were synthesized: the Rab3A effector domain peptide sequence mimicked the wild-type effector domain of Rab3A$^{52–67}$ protein (16), VSTVGIDFKVKTIYRN; the Rab3AL effector domain peptide sequence was VSALGIDFKVKTIYRN (this peptide mimics a Thr-Val for a Ala-Leu amino acid substitution in the equivalent domain of Ras that inhibits guanine nucleotide biding and hydrolysis yet has no effect in Rab3A in terms of promoting exocytosis [23,24]); the Rab4 effector domain sequence was NHTIGVEFGSKIINVY, corresponding to Rab4$^{38–51}$; the Ras effector domain synthetic peptide sequence was YDPTIEDSYRKQVVID, corresponding to H-Ras$^{32–47}$; and the photoactivatable cross-linking Rab3AL-X effector domain peptide sequence was VSALGID-Bpa-KVKTIYRN, and Rab3A-X was VSTVGID-Bpa-KVKTIYRN, where the phenylalanine in the Rab3AL and Rab3A peptides has been substituted with Bpa. The CaMK-2 peptide mimicked the conserved calmodulin-binding domain of rat CaMK-2 isoforms (25), ARRKLKGAILTTMLATRNFSG; the photoactivatable cross-linking CaMK-2-X peptide mimicked the calmodulin-binding domain of CaMK-2, YLKGAILTTMLATRN-Bpa-SG, except that the three NH_2-terminal amino acids on the CaMK-2 peptide were replaced by a tyrosine for convenient Na[^{125}I]I iodination. The Rab3AL-X, Rab3A-X, and CaMK-2-X peptides were [^{125}I]iodinated on Tyr as previously described (18), and [^{125}I]Rab3AL-X, [^{125}I]Rab3A-X, and [^{125}I]CaMK-2-X were purified by HPLC to give a postpurification specific radioactivity of ~1.8–2.0 mCi/μg peptide. Photoactivated cross-linking of Bpa-containing peptides was as previously described (18), using either rat insulinoma tissue or rat liver homogenate lysates (<2 μg total protein) or semipurified material from aliquots of column chromatography runs as indicated. Competition for [^{125}I]Rab3AL-X cross-linking was with either nonradiolabeled synthetic peptides as previously described (18) or recombinant proteins. Preparation of thrombin-cleaved GST-fusion recombinant proteins of Rab3A, Rab3AT36N, Rab3AQ81L, Rab4, Ras, and human calmodulin was as previously described (16). For pH-dependence studies, the buffering component of the cross-link buffer was changed to 50 mmol/l glycine/HCl (pH 3.0), 50 mmol/l Na acetate (pH 4.0–5.5), 50 mmol/l MES/HCl (pH 6.0/6.5), 50 mmol/l Tris/HCl (pH 7.0–8.0), or 50 mmol/l Na borate/NaOH (pH 8.5–10.0). For Ca^{2+}-dependence experiments, the cross-link buffer was prepared in standard Ca^{2+}-buffered solutions between pCa1 and pCa8 (World Precision Instruments) containing 0.1% (vol/vol) Triton X-100, 0.25% (vol/vol) Tween-20, and protease inhibitors as previously stated except for omission of EDTA (18). The cation replacement cross-link buffers consisted of 10 mmol/l Tris/HCl (pH 7.4), 10 mmol/l EDTA, 5 mmol/l divalent cation chloride, 90 mmol/l KCl, 0.1% (vol/vol) Triton X-100, 0.25% (vol/vol) Tween-20, and protease inhibitors as stated (18). Analysis of [^{125}I]Rab3AL-X, [^{125}I]Rab3A-X, or [^{125}I]CaMK-2-X cross-linking was by SDS-PAGE, autoradiography, and densitometric scanning as previously described (18). It should be noted that no difference was observed between cross-linking of [^{125}I]Rab3AL-X compared with [^{125}I]Rab3A-X.

Protein purification. Protein purification of REEP-1 and -2 proteins, which specifically cross-link to [^{125}I]Rab3AL-X (18), was achieved from rat insulinoma tissue (20) or rat liver homogenate by the same approach. Cross-linking with [^{125}I]Rab3AL-X was used as an assay to track the 17/20-kDa protein doublet through the purification procedure (18). Livers isolated from five Sprague-Dawley rats or 25 g (wet weight) of rat insulinoma tissue were Potter homogenized in 5 vol of ice-cold 0.25 mol/l sucrose, 50 mmol/l Tris/HCl (pH 7.4), 1 mmol/l EDTA, and 2 mmol/l $CaCl_2$. The homogenate was centrifuged (1,500*g* at 4°C for 5 min), and the supernatant was collected and then centrifuged at 150,000*g* (25,000 rpm Beckman SW-28 rotor at 4°C for 90 min). The supernatant containing the majority of the 17/20-kDa protein doublet was collected and subjected to $(NH_4)_2SO_4$ precipitation on ice. The protein pellet was resuspended in 50 mmol/l Tris/HCl (pH 7.4), 1 mmol/l EDTA, and 2 mmol/l $CaCl_2$ and then dialyzed against the same buffer to remove excess $(NH_4)_2SO_4$. The sample was next subjected to batchwise extraction with diethylaminoethyl (DEAE)-ion exchange resin extraction and eluted by serial salt washes. The majority of Rab3A-associated 17/20-kDa protein doublet was eluted in a 0.4–0.8 mol/l NaCl wash, which was collected, dialyzed to remove the NaCl,

and then concentrated (Amicon Centriprep-10). A series of chromatographic steps then followed using a fast-performance liquid chromatography system (Pharmacia Biotech). After each chromatography step, fractions containing the 17/20-kDa protein doublet (as determined by [^{125}I]Rab3AL-X cross-linking [18]) were collected, dialyzed, and concentrated as stated above. Column chromatography steps were as follows: *1*) DEAE-ion exchange (0–1 mol/l NaCl elution gradient); *2*) phenyl-Sepharose (0–2% [vol/vol] Triton X-100 elution gradient); *3*) fast-flow Q-Sepharose (0–1 mol/l NaCl elution gradient); *4*) monoQ anion exchange (0.4–0.8 mol/l NaCl and 0.8–1.0 mol/l NaCl two-step elution gradient); and *5*) monoQ anion exchange (0–0.6 mol/l NaCl and 0.6–1.0 mol/l NaCl two-step elution gradient). After the final column run, the fractions containing the 17/20-kDa doublet were collected, dialyzed against H_2O, and lyophilized. A small aliquot (<10%) of this preparation was analyzed for purity by gel electrophoresis and subsequent silver staining.

Microsequence analysis. After protein purification, the majority of this sample was run on SDS-PAGE (15% [wt/vol] acrylamide) and then transferred by semidry electroblotting to PVDF membrane (ProBlott; Applied Biosytems). The purified band was visualized by Coomassie staining, cut out, and trypsin, digested as described (26). A like-sized segment of membrane from a protein-free region of the blot was separately subjected to trypsinization as a background control. Tryptic peptides were purified by reverse-phase HPLC (Hewlett-Packard 1090 chromatograph, Vydac C_{18} column) as described (27). The peptides were detected by absorbance at 220 nm and collected. Automated Edman sequence analysis was performed on a Perkin-Elmer (Applied Biosystems) Model 494 Procise instrument. Matrix-assisted laser-desorption time-of-flight mass spectrometry was performed on a Voyager II instrument (Perspective Biosystems).

Immunoblot and coimmunoprecipitation analysis. Immunoblot analysis, using 50 μg total protein of each subcellular fraction or starting homogenate and chemiluminescence (Amersham) for detection, was as previously described (22). Coimmunoprecipitation analysis of the Rab3A-calmodulin association was carried out from lysates of isolated rat pancreatic islets. Immunoprecipitation using either Rab3A specific antisera (18) or nonimmune rabbit serum as a control was as previously described (22). Immunoprecipitates were eluted in electrophoresis sample buffer and run on PAGE, using recombinant Rab3A and calmodulin run as standards. Coimmunoprecipitation of calmodulin with Rab3A was detected by immunoblot. Confirmation of specific Rab3A immunoprecipitation was by GTP-γ-[^{35}S] overlay (18).

Protein-protein interaction studies. Examination of whether calmodulin acted as a GAP activity to accelerate the intrinsic GTPase activity of Rab3A was as described (28) using recombinant 0.08 μmol/l Rab3A and 0.4 μmol/l calmodulin proteins in vitro. Determination of whether recombinant calmodulin (0.5–1.2 μmol/l) had GEF activity for recombinant Rab3A (0.1–0.12 μmol/l) was assessed by both [^{3}H]GDP disassociation (28) and GTP-γ-[^{35}S] association assays (15). In these Rab3A-GEF assays, the Rab-specific GEF, MSS4 (0.5–1.2 μmol/l), was used as a positive control (15).

The nucleotide requirement for Rab3A-calmodulin interaction was evaluated as follows: Rab3A (0.6 μg [~24 pmol]) was incubated with either biotinylated calmodulin (0.4 μg [~22 pmol]) or nonbiotinylated calmodulin (0.4 μg [~22 pmol]) for 3 h at 4°C in 10 μl final volume of a buffer containing 50 mmol/l Tris-HCl (pH 7.4), 1 mmol/l $CaCl_2$, 0.5% (vol/vol), Triton-X-100 ± addition of 0.5 mmol/l ADP-β-S, ATP-γ-S, GDP-β-S, or GTP-γ-S. Then, 300 μl of 0.1 mg streptavidin magnetic particle suspension was added. The particles were prewashed three times in buffer containing 50 mmol/l Tris-HCl (pH 7.4), 1 mmol/l $CaCl_2$, 0.5% (vol/vol) Triton-X-100, 0.3 mol/l NaCl, and 2 mg/ml BSA, ± 0.5 mmol/l nucleotide as appropriate. The samples were then incubated for a further 30 min at 4°C with rotary mixing. The streptavidin magnetic particles (and associated proteins) were collected with a magnetic separation stand and washed three times in the same buffer. The particles were heated at 95°C in 20 μl electrophoresis sample buffer for 5 min. This sample was centrifuged (10,000*g* for 5 min at 25°C), and the supernatant was collected and run directly on SDS-PAGE. The amount of Rab3A associated with biotinylated calmodulin was assessed by immunoblot analysis, chemiluminescence autoradiographic detection, and densitometric scanning (22).

Similar experiments were carried out to examine whether CaMK-2, as a model calmodulin-binding protein, could act as a competitive inhibitor of the Rab3A-calmodulin association. Recombinant Rab3A (2.3 μg [~92 pmol]) was first incubated with biotinylated calmodulin (220 ng [~12 pmol]) in 10 μl final volume of 50 mmol/l Tris-HCl (pH 7.4), 1 mmol/l $CaCl_2$, 0.5% (vol/vol) Triton-X-100, and 0.5 mmol/l GTP-γ-S for 3 h at 4°C. The biotinylated calmodulin (and associated Rab3A) was then extracted and washed using streptavidin magnetic particles as described above. The streptavidin magnetic particle/biotinylated calmodulin-Rab3A complex was then resuspended in 40 μl of the same buffer containing increasing quantities (0–200 ng) of purified rat brain CaMK-2 (Calbiochem) and 12.5% (vol/vol) glycerol, and then it was incubated for a further 3 h at 4°C with continuous mixing. The streptavidin magnetic particles were collected and then heated at 95°C in 20 μl electrophoresis buffer for 5 min, and the amount of Rab3A present was assessed by SDS-PAGE and immunoblotting as described above.

Other procedures. Protein was determined by using the bicinchoninic acid method (Pierce) with BSA as standard. Free Ca^{2+} concentration was estimated from reference stability constants as described (29).

RESULTS

Specific interaction of a 17/20-kDa protein doublet with Rab3A's effector domain. It has been previously shown that the [^{125}I]Rab3AL-X peptide specifically cross-linked to a 17/20-kDa doublet in β-cells that were tentatively named REEP-1 and -2 (18). The [^{125}I]Rab3AL-X peptide cross-linking to the 17/20-kDa doublet was competitively inhibited only by nonradiolabeled, non–cross-linking Rab3A effector domain synthetic peptides ($Ki_{0.5}$ = 8–10 μmol/l) (Fig. 1*A*), suggesting that this association was specific for Rab3A's effector domain. The [^{125}I]Rab3AL-X peptide cross-linking was also subjected to competitive inhibition by Rab3A recombinant proteins, but not by related GTP-binding proteins such as Ras or Rab4 (Fig. 1*B*). Wild-type Rab3A protein or Rab3AT36N variant protein (which does not stably bind guanine nucleotides, mimicking the conformational state of "inactive" Rab3A [10]) each inhibited [^{125}I]Rab3AL-X peptide cross-linking to the 17/20-kDa doublet with a range of efficacy similar to that exhibited by Rab3A effector domain synthetic peptides ($Ki_{0.5}$ = 8–10 μmol/l) (Fig. 1*A* and *B*). The Rab3AQ81L variant protein (which is defective in GTPase activity and mimics the conformational state of Rab3A in an "active" GTP-bound state [10]) inhibited [^{125}I]Rab3AL-X peptide cross-linking to the protein doublet with even higher affinity ($Ki_{0.5} \leq 2$ μmol/l) (Fig. 1*B*). Further experiments examined competitive inhibition of [^{125}I]Rab3AL-X peptide cross-linking to the 17/20-kDa doublet by wild-type recombinant Rab3A protein (Rab3A-WT) ± 100 μmol/l GDP-β-S or GTP-γ-S. In the presence of GDP-β-S, Rab3A-WT competed for [^{125}I]Rab3AL-X cross-linking with a $Ki_{0.5}$ = 8.7 ± 1.4 μmol/l (n = 3) that was similar to Rab3A-WT in the absence of guanine nucleotide ($Ki_{0.5}$ = 7.8 ± 1.1 μmol/l [n = 3]), or Rab3AT36N (Fig. 1*B*). However, in the presence of GTP-γ-S, Rab3A-WT inhibited [^{125}I]Rab3AL-X cross-linking with greater affinity ($Ki_{0.5}$ = 2.7 ± 0.6 μmol/l [n = 3]), similar to that by Rab3AQ81 l (Fig. 1*B*). Taken together, these data suggested that the 17/20-kDa doublet has a preference to associate with Rab3A's effector domain when Rab3A is in a GTP-bound state. The quantitative similarity between the competitive inhibition for Rab3A effector synthetic peptides and recombinant Rab3A proteins suggested that this protein-protein interaction applied to full-length Rab3A protein and was not necessarily an artifact associated with the use of synthetic peptides.

Identification of the protein doublet interacting with the Rab3A effector domain as calmodulin. The identity of the 17/20-kDa protein doublet was determined by its purification, using [^{125}I]Rab3AL-X peptide cross-linking as an assay, and subsequent microsequencing. It was found that this protein doublet was expressed in most rat tissues, and purification was achieved to a single silver-stained ~18 kDa band resolved on gel electrophoresis from the NEDH rat transplantable insulinoma (18). Automated Edman sequence analysis of three tryptic peptides from

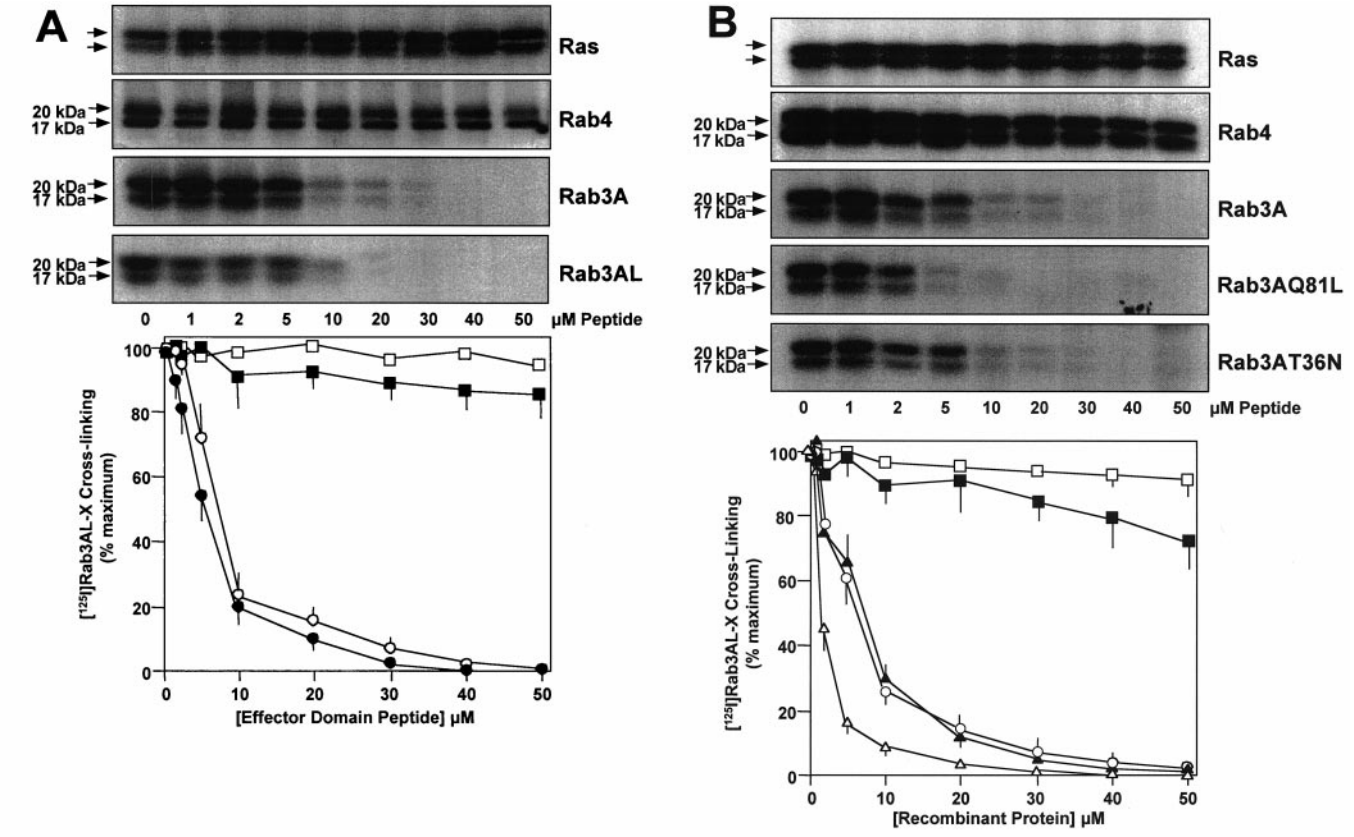

FIG. 1. A 17/20-kDa protein doublet specifically interacts with Rab3A effector domain peptides and recombinant proteins. Specific competitive inhibition of photoactivated cross-linking of [^{125}I]Rab3AL-X to a 17/20-kDa cytosolic protein doublet in rat insulinoma tissue lysate (2 μg total protein) by either "effector domain" synthetic peptides (*A*) or recombinant Rab3A-related fusion proteins (*B*) was performed as previously described, with analysis by gel electrophoresis, autoradiography, and densitometric scanning. □, Ras; ■, Rab4; ○, Rab3A; ●, Rab3AL; △, Rab3AQ81L; ▲, Rab3AT36N. Each panel contains a specimen autoradiograph for each competitive agent, and a graph of densitometric scanning analyses. Results are means ± SE of at least three independent determinations.

a digest of the purified protein (denoted T1, T2, and T4) revealed amino acid sequences of ELGTVMR for T1 (equivalent to rat calmodulin$^{31–37}$ [30]), VFDKDG for T2 (equivalent to rat calmodulin$^{91–96}$ [30]), and HVMTNLGEX-LTDEEQIAEFK for T4 (equivalent to rat calmodulin$^{107–126}$ [30], where X indicates ϵ *N*,*N*,*N*-trimethyllysine at rat calmodulin^{115}). Furthermore, a fourth tryptic peptide, designated T3, gave no sequence and appeared to be NH_2-terminally blocked. However, matrix-assisted laser desorption mass spectrometry of this peptide gave MH^+ of 1,564.9, in agreement with the theoretical value for the predicted NH_2-terminal tryptic peptide of rat calmodulin, α-*N*-acetyl-ADQLTEEQIAEFK (30). A further detail emerged from sequencing of tryptic peptide T2. After six Edman cycles had given a result of VFDKDG, consistent with rat calmodulin$^{91–96}$ amino acid sequence, the seventh cycle reported an abrupt decline in signal strength as the sequencing continued. Signals were detected for both Asn (the expected residue 97 of rat calmodulin [30]) and Asp, after which the sequence signal continued at a diminished level, yielding a result of GYISAAELR that matched rat calmodulin$^{98–106}$ (30). The result suggested extensive deamidation of Asn^{97} to Asp, with an additional fraction of this residue converted to isoaspartate and consequently losing its susceptibility to Edman degradation. There was also a 50% drop in sequence signal strength from the fifth to the sixth cycles, consistent with partial isoaspartate formation at Asp^{95}. These results complement observations previously made for bovine brain calmodulin (31) and provide a good explanation for detection of calmodulin from rat insulinoma as a 17/20-kDa doublet detected on electrophoretic analysis of [^{125}I]Rab3AL-X peptide cross-linking (18) (Figs. 1 and 2) as representing amidated/deamidated forms of calmodulin. A similar doublet was observed for purified bovine calmodulin subjected to cross-linking with [^{125}I]Rab3AL-X peptide (data not shown).

Ca^{2+}, pH, and GTP dependence of the Rab3A-calmodulin interaction. The association between the effector domain of Rab3A and calmodulin was pH-dependent (Fig. 2*A*). Significant cross-linking of peptide to calmodulin was between pH 6.5 and 8.0, with an optimum pH between 7.0 and 7.5 (Fig. 2*A*), and thus it was ideally suited to β-cell's cytosolic environment. The interaction between Rab3A's effector domain and calmodulin was also Ca^{2+}-dependent (Fig. 2*B*). The chelating agents EDTA and EGTA both inhibited [^{125}I]Rab3AL-X peptide cross-linking to endogenous calmodulin in an insulinoma cell lysate (Fig. 2*B*). However, with increasing Ca^{2+} concentrations (between 1 μmol/l and 1 mmol/l Ca^{2+}) (Fig. 2*B*), [^{125}I]Rab3AL-X peptide cross-linking to calmodulin could be regained at a maximum at 100 μmol/l Ca^{2+}. The $K_{0.5}$ maximal activation of the interaction between the Rab3A effector domain and calmodulin was 14.6 ± 1.1 μmol/l Ca^{2+} (mean ± SE [n = 8]) for endogenous calmodulin in an insulinoma cell lysate (Fig. 2*B*). The interaction of Rab3A's effector domain with calmodulin was strictly Ca^{2+}-dependent, since no other

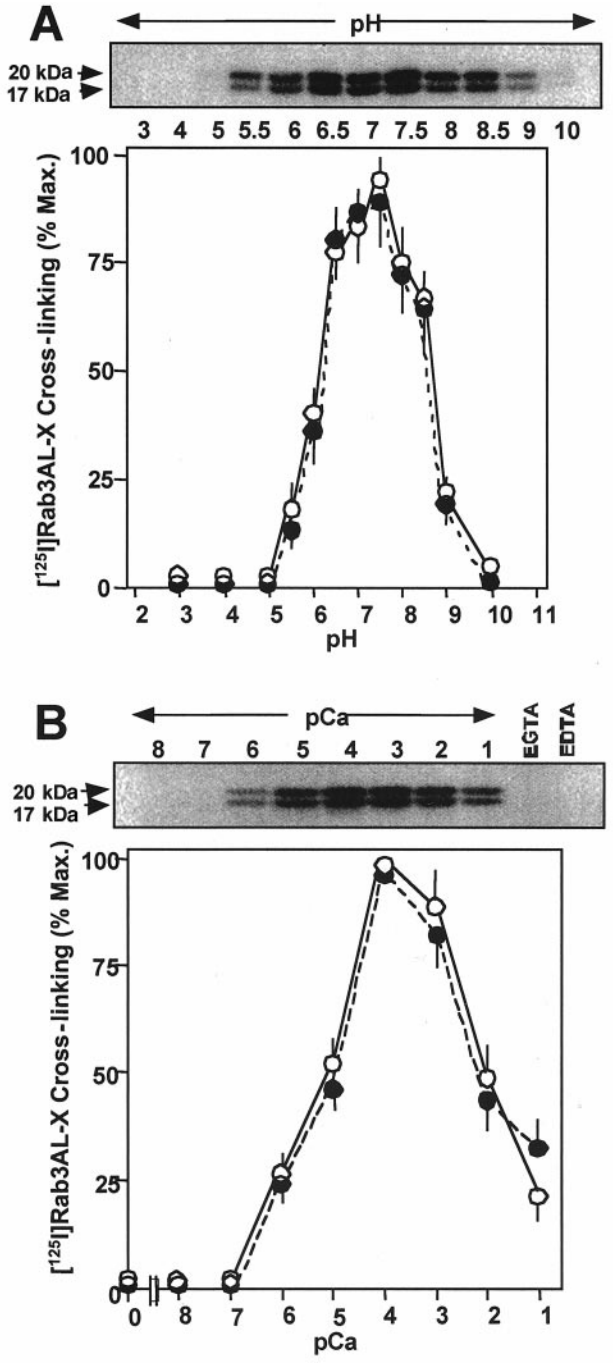

FIG. 2. Rab3A effector domain interaction with calmodulin is pH- and Ca^{2+}-dependent. Specific photoactivated cross-linking of [^{125}I]Rab3AL-X to calmodulin was determined at a pH between 3.0 and 10.0 in rat insulinoma tissue lysate ([*A*] 1 μg total protein). Ca^{2+} dependence of [^{125}I]Rab3AL-X cross-linking to calmodulin was determined at pH 7.0 between 1 and 8 pCa in rat insulinoma tissue lysate ([*B*] 1 μg total protein). A very similar pH profile and Ca^{2+} dependence were found using 25 ng purified bovine calmodulin (data not shown). A sample autoradiograph is shown in each instance, with a graph of densitometric scanning analyses. ○, 20 kDa; ●, 17 kDa. Results are means ± SE of at least three independent determinations.

divalent cation (including Mg^{2+}, Mn^{2+}, Ba^{2+}, Ni^{2+}, Sr^{2+}, Cu^{2+}, Zn^{2+}, Co^{2+}, or Cd^{2+}) could significantly restore [^{125}I]Rab3AL-X peptide cross-linking calmodulin after EDTA chelation (data not shown). The pH profile and Ca^{2+} dependence for Rab3A effector domain interaction with purified bovine calmodulin was essentially the same as that for calmodulin in the insulinoma lysate (data not shown). This further validated the identity of the 17/20-kDa doublet as rat calmodulin.

In addition to Ca^{2+} and pH dependence, the Rab3A-calmodulin interaction was preferred when Rab3A was in a GTP-bound state (Fig. 3). Incubation of biotinylated calmodulin with Rab3A under optimal in vitro conditions (i.e., pH 7.4/1 mmol/l $CaCl_2$), followed by streptavidin-magnetic particle extraction and Rab3A immunoblot analysis, revealed a more than fourfold increase in Rab3A associated with biotinylated calmodulin in the presence of GTP-γ-S, compared with no nucleotide, ADP-β-S, ATP-γ-S, or GDP-β-S addition (Fig. 3). When nonbiotinylated calmodulin was used, negligible Rab3A was detected by subsequent immunoblot analysis, irrespective of the nucleotide present (Fig. 3). These results complemented the observations of a preferred calmodulin interaction with the Rab3AQ81L variant (Fig. 1*B*).

Rab3A was located on β-granules and the Rab3A-calmodulin interaction inversely correlated with glucose-induced insulin secretion in isolated pancreatic islets. Subcellular fractionation of insulinoma cells, followed by immunoblotting analysis of cytosolic-, β-granule–, and plasma membrane–enriched fractions, indicated that the majority of Rab3A and a detectable proportion of calmodulin in pancreatic β-cells were colocalized to β-granules (Fig. 4*A*). Unlike Rab3A's predominant location to β-granules, calmodulin was also found in both the cytosolic and plasma membrane fractions. Detectable CaMK-2 isoform was also found on β-granules; however, the majority was located to the plasma membrane, with little detected in the cytosolic fraction (Fig. 4*A*). The Rab-specific GEF, MSS4 (15), was found to be a cytosolic protein (Fig. 4*A*). It was examined whether a Rab3A-calmodulin association occurred in pancreatic islet β-cells in vivo, in a manner that correlated with regulated insulin secretion. Insulin exocytosis from pancreatic β-cells is regulated by nutrients, including glucose and fatty acids (1). Specific immunoprecipitation of Rab3A from rat pancreatic islet cell lysates followed by calmodulin immunoblot analysis revealed that a specific Rab3A-calmodulin interaction was apparent in vivo (Fig. 4*B*). Nonimmune serum did not immunoprecipitate Rab3A, as detected by subsequent GTP-γ-[^{35}S] overlay, and consequently only nonspecific "background" calmodulin was detected by subsequent immunoblot analysis (Fig. 4*B*). Specific Rab3A immunoprecipitation from islets incubated under conditions of basal insulin secretion at 2.8 mmol/l glucose re-

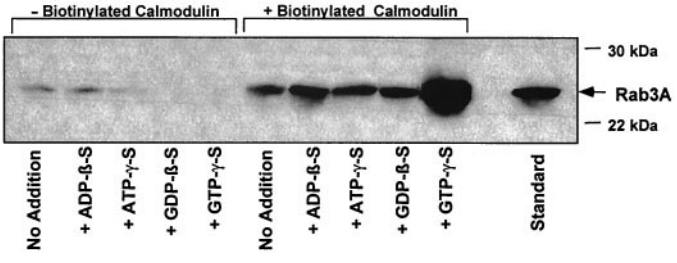

FIG. 3. Rab3A-calmodulin interaction is preferred when Rab3A is in a GTP-bound state. The association of recombinant Rab3A and calmodulin (biotinylated or nonbiotinylated) at pH 7.4 and 1 mmol/l $CaCl_2$ was assessed in either the absence or presence of 0.5 mmol/l ADP-β-S, ATP-γ-S, GDP-β-S, or GTP-γ-S as described previously. A typical immunoblot analysis of the amount of Rab3A associated with biotinylated calmodulin is shown.

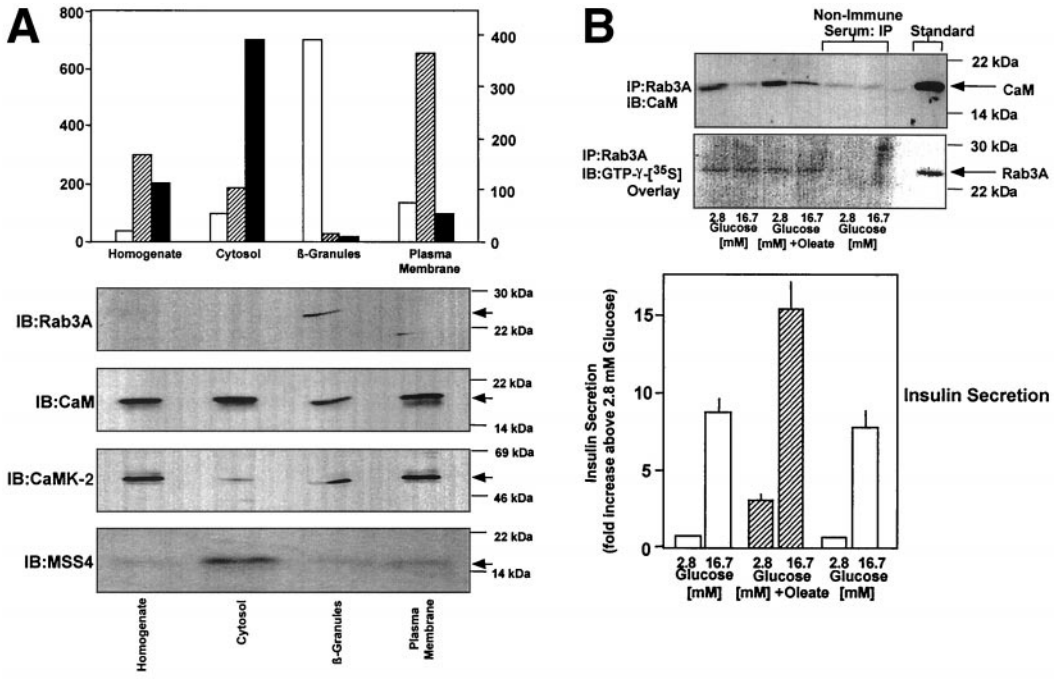

FIG. 4. Rab3A and calmodulin are colocalized on insulin secretory granules and interact in vivo in a manner that inversely correlated with nutrient-regulated insulin exocytosis. *A*: Immunoblot analysis and preparation of insulinoma subcellular fractions enriched for insulin secretory granules, plasma membrane, and cytosol were as described. Increased specific activity of marker enzyme analysis over the starting insulinoma tissue homogenate indicated significantly enriched insulin secretory granule (insulin as "marker enzyme"), cytosolic (lactate dehydrogenase [LDH] as marker enzyme), and plasma membrane (5′-nucleotidase as marker enzyme) subcellular fractions. □, Insulin specific activity (ng/μg protein); ▨, 5′-nucleotidase specific activity (μmol/min/μg protein); ■, LDH specific activity (μmol/min/μg protein). *B*: Coimmunoprecipitation of calmodulin with rab3A in vivo. Specific Rab3A immunoprecipitation (IP) and subsequent immunoblot analysis (IB) for calmodulin and rab3A detection by GTP-γ-[^{35}S] overlay were as described previously. A typical immunoblot analysis of triplicate experiments is shown. Nonimmune rabbit serum was used for control immunoprecipitation, and consequently, only very low background levels of calmodulin could be detected, and no Rab3A was detected, as indicated by GTP-γ-[^{35}S] overlay. Insulin secretion was assayed from the same isolated islet incubations. Under conditions of basal insulin secretion at 2.8 mmol/l glucose, 0.09% insulin content was released per hour; at 16.7 mmol/l glucose-induced insulin secretion, 0.77% insulin content released per hour. □, indicates in the absence of oleate; ▨, indicates in the presence of oleate (125 μmol/l complexed to 0.1% BSA). The secretion data are means ± SE of three observations.

vealed a distinct calmodulin interaction with Rab3A above background (Fig. 4*B*). Upon stimulation of insulin secretion by 16.7 mmol/l glucose, calmodulin-Rab3A interaction dissociated (Fig. 4*B*). Addition of the fatty acid oleate potentiated both basal and glucose-induced insulin secretion (Fig. 4*B*), as previously observed (1). In the presence of oleate, the Rab3A-calmodulin interaction at a basal 2.8 mmol/l glucose was still apparent, and it dissociated upon increasing the glucose concentration to a stimulatory 16.7 mmol/l glucose to a similar extent as observed in the absence of oleate (Fig. 4*B*).

Calmodulin does not affect the GTPase activity or guanine nucleotide exchange of Rab3A. The characteristics of the calmodulin-Rab3A interaction were further investigated. Calmodulin did not affect the intrinsic GTPase activity of Rab3A (Fig. 5*A*), so it was unlikely that it was acting as a Rab3A-specific GAP activity. Moreover, calmodulin did not affect guanine nucleotide exchange for Rab3A as measured by either the rate of GDP release from Rab3A (Fig. 5*B*) or GTP association to Rab3A (Fig. 5*C*). As a positive control, recombinant MSS4 clearly accelerated GDP release/GTP association toward Rab3A, as previously observed (15). Calmodulin did not affect the GEF activity of MSS4 directed at Rab3A (Fig. 5*B* and *C*).

Differential Ca^{2+} dependence of calmodulin interaction with Rab3A versus CaMK-2. The association of recombinant human calmodulin to the Rab3A effector domain (using [^{125}I]Rab3A-X photoreactive cross-linking peptide) was compared with a model of a typical calmodulin-binding protein, the calmodulin-binding domain of CaMK-2 (25,32), using [^{125}I]CaMK-2-X photoreactive cross-linking peptide. Chelating agents EDTA and EGTA both inhibited [^{125}I]Rab3A-X and [^{125}I]CaMK-2-X peptide cross-linking calmodulin (Fig. 6), similarly to that of [^{125}I]Rab3AL-X (Fig. 2*B*). However, with increasing Ca^{2+} concentrations, detectable amounts of [^{125}I]Rab3A-X peptide cross-linking to calmodulin could be regained between 1 and 10 μmol/l [Ca^{2+}], reaching a maximum at 100 μmol/l [Ca^{2+}] (Fig. 6). The $K_{0.5}$ maximal activation of the association between the Rab3A effector domain and calmodulin was 15.4 ± 1.3 μmol/l [Ca^{2+}] (mean ± SE [$n = 4$]) (Fig. 6), similar to that for bovine and rat calmodulin (Fig. 2*B*). [^{125}I]CaMK-2-X peptide cross-linking to calmodulin showed a Ca^{2+} dependence different from that for [^{125}I]Rab3A-X peptide (Fig. 6). Detectable calmodulin association to [^{125}I]CaMK-2-X was observed between 10 and 100 μmol/l [Ca^{2+}], reaching a maximum >1 mmol/l [Ca^{2+}] (Fig. 6). The $K_{0.5}$ maximal activation of the association between the CaMK-2 peptide and human calmodulin was 37.6 ± 4.9 μmol/l [Ca^{2+}] (mean ± SE [$n = 4$]) (Fig. 6), comparable to that observed for CaMK-2 activation (33). At >100 μmol/l [Ca^{2+}], the calmodulin interaction with CaMK-2-X peptide remained relatively stable compared with that with Rab3A-X peptide, which tended to dissociate at higher [Ca^{2+}] (Fig. 6).

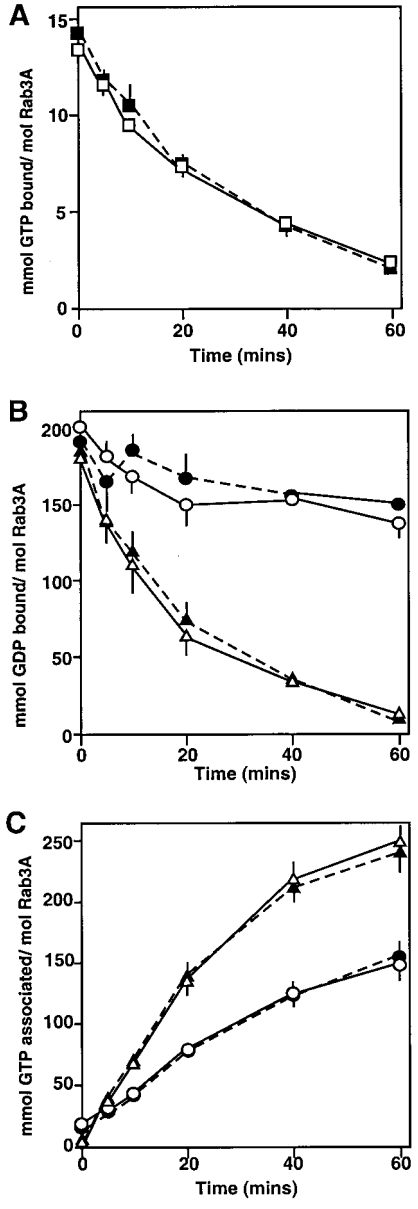

FIG. 5. Calmodulin does not affect GTPase activity or GEF activity toward Rab3A. *A*: The GTPase activity of Rab3A (0.08 μmol/l) was measured in vitro in the absence (□) or presence (■) of calmodulin (0.4 μmol/l) for up to 60 min at 30°C as described previously. The effect of calmodulin on GEF activity toward Rab3A GTPase activity of Rab3A was measured in vitro as either GDP dissociation (*B*) or GTP association (*C*), as described previously. For the GDP dissociation assay (*B*), 0.12 μmol/l Rab3A ± 1.2 μmol/l calmodulin and/or 1.2 μmol/l MSS4 was incubated for up to 60 min at 30°C. For the GTP association assay (*C*), 0.1 μmol/l Rab3A was incubated with 0.5 μmol/l calmodulin and/or 0.5 μmol/l MSS4 for up to 60 min at 30°C. Incubation of Rab3A alone (○), plus calmodulin (●), plus MSS4 (△), and plus calmodulin and MSS4 (▲) are shown. All results are means ± SE of at least three independent determinations.

Differential affinity of the calmodulin interaction with Rab3A versus CaMK-2. Competitive inhibition by Rab3A and CaMK-2 synthetic peptides (1 nmol/l to 100 μmol/l) for cross-linking of [^{125}I]Rab3A-X or [^{125}I]CaMK-2-X to recombinant human calmodulin was assessed over a range of [Ca^{2+}] (Table 1). Titration inhibition curves were then constructed, from which $Ki_{0.5}$ (the concentration of Rab3 or CaMK-2 that rendered 50% inhibition of [^{125}I]Rab3A-X or [^{125}I]CaMK-2-X cross-linking to calmodulin) was calculated (Table 1). The $Ki_{0.5}$ of Rab3A peptide inhibition

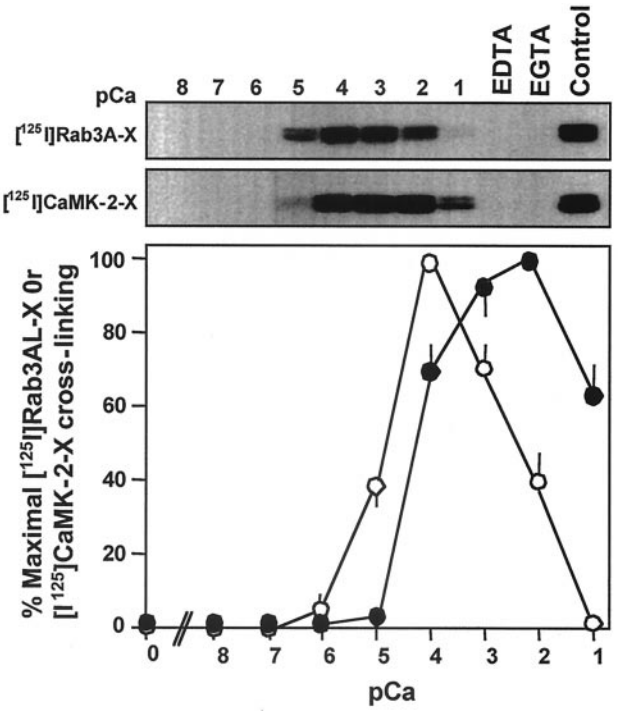

FIG. 6. Different Ca^{2+} dependence of calmodulin association with the Rab3A effector domain and calmodulin-binding domain of CaMK-2. Specific photoactivated cross-linking of [^{125}I]Rab3A-X or [^{125}I]CaMK-2-X peptides to recombinant human calmodulin (25 ng) was determined at pH 7.0 between 1 and 8 pCa as described previously. A sample autoradiograph is shown in each instance, with a graph of densitometric scanning analysis of [^{125}I]Rab3A-X (○) and [^{125}I]CaMK-2-X (●) depicted, where results are means ± SE of at least three independent determinations.

was lowest at 100 μmol/l [Ca^{2+}] for [^{125}I]Rab3A-X and [^{125}I]CaMK-2-X cross-linking to calmodulin (Table 1), indicative of the optimal Ca^{2+} dependence for Rab3A-calmodulin interaction (Figs. 2*B* and 6). The CaMK-2 synthetic peptide inhibited [^{125}I]Rab3A-X and [^{125}I]CaMK-2-X cross-linking to calmodulin, with a $Ki_{0.5}$ between 40 and 400 nmol/l, depending on the [Ca^{2+}] (Table 1). The $Ki_{0.5}$ of CaMK-2 peptide inhibition was lowest at 1 mmol/l [Ca^{2+}] for both [^{125}I]Rab3A-X and [^{125}I]CaMK-2-X cross-

TABLE 1
Competitive inhibition of [^{125}I]Rab3AL-X or [^{125}I]CaMK-2-X cross-linking to calmodulin by Rab3A and CaMK-2 peptides

Cross-linking peptide	[Ca^{2+}] (mol/l)	$Ki_{0.5}$ for competing peptide	
		Rab3A (μmol/l)	CaMK-2 (nmol/l)
[^{125}I]Rab3AL-X	10^{-5}	22.6 ± 3.2	389 ± 51
	10^{-4}	5.3 ± 0.8	165 ± 24
	10^{-3}	8.2 ± 1.5	122 ± 37
[^{125}I]CaMK-2-X	10^{-5}	17.8 ± 1.3	293 ± 37
	10^{-4}	5.2 ± 0.7	87 ± 12
	10^{-3}	9.4 ± 2.1	42 ± 7

Data are means ± SE of at least three independent determinations. Competitive inhibition by Rab3A and CaMK-2 synthetic peptides (1 nmol/l–100 μmol/l) for recombinant calmodulin cross-linking to [^{125}I]Rab3A-X or [^{125}I]CaMK-2-X peptides was assessed over a Rab3A/CaMK-2 concentration range at 10 μmol/l, 100 μmol/l, and 1 mmol/l [Ca^{2+}] as described in RESEARCH DESIGN AND METHODS. From these experiments, titration inhibition curves could be constructed, from which a $Ki_{0.5}$ the concentration of Rab3 or CaMK-2 that rendered 50% inhibition of [^{125}I]Rab3A-X or [^{125}I]CaMK-2-X cross-linking to calmodulin) could be calculated.

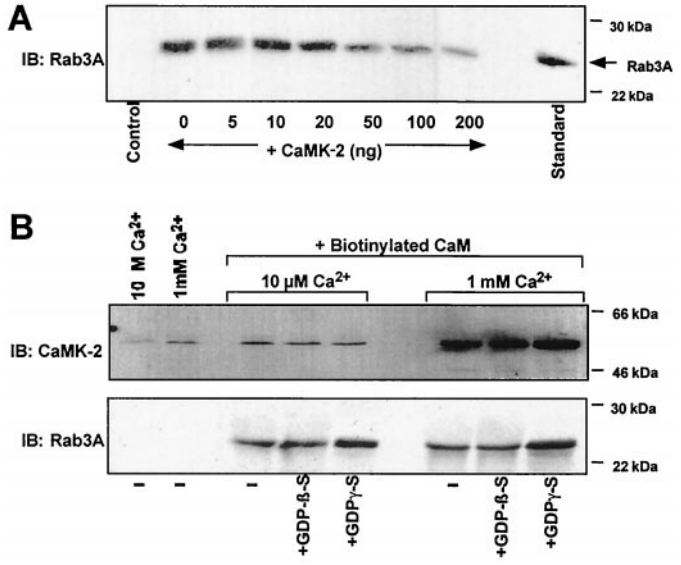

FIG. 7. CaMK-2 competes for calmodulin prebound to Rab3A. *A*: Recombinant Rab3A was prebound to biotinylated calmodulin (or nonbiotinylated as a control) under optimal conditions of pH 7.4, 1 mmol/l $CaCl_2$, and 0.5 mmol/l GTP-γ-S and extracted with streptavidin magnetic particles as described previously. The Rab3A-calmodulin complex was then incubated with increasing amounts of purified rat brain CaMK-2 (0–200 ng), pH 7.4, and 1 mmol/l $CaCl_2$, reextracted with streptavidin magnetic particles, and analyzed for the amount of Rab3A remaining associated with biotinylated calmodulin by immunoblotting. A typical immunoblot analysis is shown, in which the control was where nonbiotinylated calmodulin was used, and recombinant Rab3A was used as a standard. *B*: Biotinylated calmodulin was added to an isolated β-granule fraction under conditions of low 10 μmol/l [Ca^{2+}] or high 1 mmol/l [Ca^{2+}] ± 0.2 mmol/l GDP-β-S or 0.2 mmol/l GTP-γ-S, as indicated previously. As a control, nonbiotinylated calmodulin was added. Biotinylated calmodulin was extracted, and associated CaMK-2 and Rab3A, endogenous to β-granules, were detected by immunoblot analysis. A typical blot analysis is shown.

linking to calmodulin (Table 1), indicative of the optimal Ca^{2+} dependence for the CaMK-2/calmodulin interaction (Fig. 6). A $Ki_{0.5}$ of 40 nmol/l for CaMK-2 peptide inhibition of [^{125}I]CaMK-2-X cross-linking to calmodulin was equivalent to a previously estimated EC_{50} for CaMK-2 activation by calmodulin (34).

Calmodulin's interaction with Rab3A is competed for by CaMK-2. Recombinant Rab3A-WT was preassociated to biotinylated calmodulin under optimal conditions of 100 μmol/l [Ca^{2+}] and 50 μmol/l GTP-γ-S, and only the Rab3A specifically associated with biotinylated calmodulin was extracted using streptavidin magnetic particles. The biotinylated calmodulin-Rab3A complex was then incubated with purified rat brain CaMK-2, and then the streptavidin magnetic particles were resedimented and analyzed for the amount of Rab3A remaining associated with biotinylated calmodulin by immunoblotting. As a control, nonbiotinylated calmodulin was used, which was unable to extract any detectable Rab3A. With increasing amounts of CaMK-2 protein (>20 ng), less Rab3A association with biotinylated calmodulin was detected (Fig. 7*A*), indicating that CaMK-2 could "steal" calmodulin previously bound to Rab3A. It was also examined whether the endogenous Rab3A and CaMK-2 on isolated β-granules could compete for added biotinylated calmodulin, at either a low 10 μmol/l [Ca^{2+}] or a high 1 mmol/l [Ca^{2+}] ± GDP-β-S or GTP-γ-S (Fig. 7*B*). In the absence of added biotinylated calmodulin, negligible Rab3A and only a small amount of CaMK-2 were detected (Fig. 7*B*). This observation was considered nonspecific background. At a lower 10 μmol/l [Ca^{2+}], significant β-granule Rab3A association with biotinylated calmodulin was observed, which was increased a further two- to threefold in the presence of GTP-γ-S (Fig. 7*B*). Rab3A association with biotinylated calmodulin at the higher 1 mmol/l [Ca^{2+}], in the absence of guanine nucleotide or in the presence of GDP-β-S, did not significantly increase compared with that at lower [Ca^{2+}] (Fig. 7*B*). In the presence of GTP-γ-S, Rab3A association with biotinylated calmodulin only increased by ~30% at 1 mmol/l [Ca^{2+}] compared with that at lower 10 μmol/l [Ca^{2+}] (Fig. 7*B*). In contrast, in the same biotinylated calmodulin–extracted β-granule samples incubated at a low 10 μmol/l [Ca^{2+}], immunoblot analysis of calmodulin-associated CaMK-2 was small and only marginally above background levels (Fig. 7*B*). However, with β-granules incubated at a higher [Ca^{2+}], an eightfold increase in CaMK-2 associated with biotinylated calmodulin was detected compared with that at a lower [Ca^{2+}] (Fig. 7*B*). Association of β-granule CaMK-2 with biotinylated calmodulin was unaffected by the addition of GDP-β-S or GTP-γ-S. The differential Ca^{2+} dependence of calmodulin association with β-granule Rab3A or CaMK-2 (Fig. 7*B*) was qualitatively comparable with that found with calmodulin-binding domain peptides of Rab3A and CaMK-2 (Fig. 6).

DISCUSSION

Rab3A as a member of the family of calmodulin-binding proteins. By using a peptide cross-linking approach and coimmunoprecipitation in pancreatic islets, we have found that Rab3A is capable of a specific Ca^{2+}-dependent interaction with calmodulin via its effector domain. A Rab3A-calmodulin interaction has been previously described in neuroendocrine cells, including pancreatic β-cells, and was competed for by a synthetic peptide that partially overlapped with the Rab3A effector domain (13, 14). In this study, it was found that calmodulin interacted with Rab3A's effector domain, preferably in a GTP-bound conformation, consistent with this motif being accessible on the outside of the Rab3A molecule when in a GTP-bound activated state (16,17). A primary consensus sequence of a "calmodulin-binding domain" has been suggested for proteins that specifically interact with calmodulin (25,32). Such a motif requires a conserved basic amino acid that is analogous to a residue necessary for calmodulin to activate myosin light-chain kinase and several conserved hydrophobic amino acids (25,32). The effector domain of Rab3A aligns to this homology with a basic residue at Lys^{60} and hydrophobic residues at Val^{52}, Val^{55}, and Val^{61} (35), suggesting Rab3A as a member of the calmodulin-binding protein family (25,32). However, it should be noted that the affinity of calmodulin to associate with Rab3A was relatively weak (K_d ~5 μmol/l at 100 μmol/l [Ca^{2+}]) compared with that of more recognized calmodulin-binding proteins, such as CaMK-2 (K_d ~100 nmol/l at 100 μmol/l [Ca^{2+}]), which was used as a model calmodulin-binding protein in this study. It follows, therefore, that there are other structural considerations of the Rab3A molecule that contribute to its GTP/Ca^{2+}-dependent interaction with calmodulin. Such a relatively low-affinity calmodulin-Rab3A interaction resulted in Rab3A-bound calmodulin being readily competed for by other calmodulin-binding

proteins that have a higher affinity for calmodulin (e.g., CaMK-2), particularly as the local $[Ca^{2+}]_i$ fluctuates. This in itself may not necessarily be unimportant in terms of Rab3A's role in the mechanism of insulin exocytosis, as suggested below. Notwithstanding, as far as we have been able to determine, calmodulin was the only protein in β-cell extracts that interacted with Rab3A's effector domain. This is consistent with the failure of other Rab3A-interacting proteins, rabphilin3A, RIM, MSS4, and RabGDI, to compete for calmodulin association with Rab3A in the β-cell, and these other proteins probably associate with alternative Rab3A motifs (14).

GTP dependence of the Rab3A-calmodulin interaction in relation to GTP-induced insulin exocytosis. As well as $[Ca^{2+}]$, GTP can also induce insulin secretion from semipermeabilized β-cells (18,36). It was interesting to note that although the calmodulin-Rab3A interaction was Ca^{2+}-dependent, there was also a preference for calmodulin to interact with GTP-bound Rab3A. However, the calmodulin-Rab3A interaction did not affect GTPase activity or guanine nucleotide exchange activity of Rab3A, further implicating calmodulin as a Rab3A effector protein in β-cells. In this regard, it should be noted that calmodulin had a preference to associate with a constitutively active GTP-bound form of Rab3A (Rab3AQ81L). Interestingly, overexpression of Rab3AQ81L in pancreatic β-cells inhibits its Ca^{2+}-evoked exocytosis (37), as it does in other neuroendocrine cells (10), and has recently been attributed to Rab3A's specific interaction with calmodulin (14). As such, it has been proposed that the Rab3A/calmodulin complex has a negative role in controlling Ca^{2+}-induced insulin exocytosis by limiting the number of insulin exocytotic events (14). This notion tends to inversely correlate with the observation in Rab3A knockout mice, where Rab3A regulation of Ca^{2+}-evoked exocytosis is lost, resulting in a higher number of exocytotic events (9). Nevertheless, the Rab3A-calmodulin interaction provides a means by which Ca^{2+} and GTP can act in concert at a step in the insulin exocytotic mechanism.

Ca^{2+}-dependent Rab3A-calmodulin interaction in relation to Ca^{2+}-induced insulin exocytosis. The finding that Rab3A's effector domain is capable of a specific Ca^{2+}-dependent interaction with calmodulin indicated a degree of novel insight into the mechanism of glucose-induced insulin exocytosis. A rise in cytosolic $[Ca^{2+}]_i$, which occurs as a consequence of increased glucose metabolism in the β-cell, is one of the secondary coupling factors needed to trigger insulin exocytosis (1). Rab3A has been implicated to play a role in the mechanism of regulated exocytosis in neuroendocrine cells (6,38), including pancreatic β-cells (37). Considering that calmodulin is a key Ca^{2+}-sensing protein (25,32), the Ca^{2+}-dependent interaction of Rab3A and calmodulin provides a downstream connection between an intracellular secondary messenger (i.e., $[Ca^{2+}]_i$) and the exocytotic machinery of the pancreatic β-cell. Indeed, the Ca^{2+}-dependent Rab3A-calmodulin association occurred in a similar $[Ca^{2+}]$ range (1–100 μmol/l) required to evoke insulin secretion from semipermeabilized β-cells (18,36). This is supportive of the concept that a Rab3A-calmodulin interaction is physiologically relevant to the mechanism of Ca^{2+}-dependent insulin exocytosis. Moreover, it should be noted that other Ca^{2+}-dependent exocytotic proteins operate in the same 1–100 μmol/l $[Ca^{2+}]$ range. For example, syncollin and Ca^{2+}-dependent activator protein for secretion (CAPS) require >10 μmol/l $[Ca^{2+}]$ to evoke their regulatory role in dense-core secretory granule exocytosis (39,40). Also, Ca^{2+}-dependent binding of synaptotagmin to syntaxin has a $K_{0.5}$ of ~200 μmol/l (41), synaptotagmin binding to phospholipids only takes place at $[Ca^{2+}]$ >5 μmol/l (42), and the threshold for synaptotagmin oligomerization in exocytotic fusion pore formation requires $[Ca^{2+}]$ in the 10–100 μmol/l range (43). However, upon nutrient stimulation of intact β-cells, the *total* cytosolic $[Ca^{2+}]_i$ has been measured to rise from a resting concentration of ~50–100 to ~300 nmol/l (44), which is below the $[Ca^{2+}]$ requirement for the Rab3A-calmodulin interaction. Yet it should be considered that such measurements of cytosolic $[Ca^{2+}]$ in intact cells represent an estimate of the average $[Ca^{2+}]$ across the whole cell cytoplasm, and they do not account for local oscillatory changes in $[Ca^{2+}]$ in limited pockets of the β-cell cytosol (4). In this respect, it is important to note that L-type Ca^{2+} channels (the appropriate Ca^{2+} channel responsible for elevating cytosolic $[Ca^{2+}]$ and triggering Ca^{2+}-dependent insulin release in β-cells) (2) are associated with β-granules at the site of exocytosis (45). As such, the local $[Ca^{2+}]_i$ in the vicinity of the β-granule at the site of exocytosis is likely to be much higher than that estimated for the cytosol as a whole once L-type Ca^{2+} channels are opened. This consideration therefore provides a plausible explanation for the discrepancy between the measurements of cytosolic $[Ca^{2+}]$ in intact β-cells and the $[Ca^{2+}]$ required to trigger insulin release in semipermeabilized β-cells (36). Moreover, it suggests that the Rab3A-calmodulin interaction can occur at the site of exocytosis in the β-cell during a transient rise in local $[Ca^{2+}]_i$, as proposed for a role of Rab3A late in the exocytotic mechanism (11). However, the in vivo situation is likely more complex when it is considered that other calmodulin-binding proteins will compete with Rab3A for a calmodulin interaction which, in turn, can be influenced by the local $[Ca^{2+}]_i$ and the guanine nucleotide–binding state of Rab3A. This is underscored in the observation that various calmodulin-binding proteins, such as Rab3A and CaMK-2, have different Ca^{2+} dependencies for calmodulin association (Fig. 6).

The Rab3A-calmodulin interaction may provide a means of directing calmodulin to β-granules. The precise role for a Rab3A-calmodulin interaction in the mechanism of insulin exocytosis is, for the moment, undefined. It has been postulated that a Rab3A-calmodulin association in β-cells might act as a negative regulator of Ca^{2+}-induced insulin release to control the number of exocytotic events (14). However, such a negative influence would have to be overcome for insulin exocytosis to proceed. Indeed, this was indicated by the Rab3A-calmodulin association in islet β-cells inversely correlating with glucose-induced insulin secretion (Fig. 4*B*), associated with a translocation of calmodulin to the cytosol and disassociation with Rab3A (18). Indeed, this is somewhat similar to previous observations in neuronal cells in which calmodulin association with Rab3A under Ca^{2+}-stimulated conditions destabilizes its interaction with synaptic vesicle membranes (13). As Rab3A is mostly localized to β-granules in the β-cell (37), one possibility is that the

Rab3A-calmodulin interaction may represent a step in the mechanism of insulin exocytosis, which directs calmodulin to the cytoplasmic face of a β-granule membrane. However, it should be considered that the association of calmodulin with Rab3A is regulated by fluxes in local $[Ca^{2+}]_i$ and/or the GTP/GDP-bound state of Rab3A, and it is likely to be transient. Moreover, the Rab3A-calmodulin interaction is probably in competition with other Ca^{2+}/calmodulin-binding proteins present on β-granules. In this study, by using the calmodulin-binding site of CaMK-2 as a model calmodulin-binding protein, it was found that the Rab3A-calmodulin interaction could overlap with that of other calmodulin-binding proteins. CaMK-2 had a greater affinity for calmodulin than Rab3A, especially at higher $[Ca^{2+}]$ (Table 1). However, calmodulin's interactions with Rab3A and CaMK-2 were interchangeable. The Rab3A effector domain competitively inhibited CaMK-2–calmodulin association, and correspondingly, the CaMK-2 calmodulin-binding domain competed for the Rab3A-calmodulin interaction (Table 1). Moreover, at higher $[Ca^{2+}]$, CaMK-2 was able to readily compete for calmodulin already bound to Rab3A in vitro (Fig. 7). As an aside, and peculiar to CaMK-2, it should be noted that in vivo, at higher $[Ca^{2+}]$, activated CaMK-2 would be autophosphorylated, which markedly increases its affinity for calmodulin and, in turn, boosts its ability to "steal" calmodulin from Rab3A. Additionally, it was observed that the Rab3A-calmodulin and CaMK-2–calmodulin interactions differed in their requirements for $[Ca^{2+}]$. The threshold of $[Ca^{2+}]$ required to initiate a Rab3A-calmodulin association was lower than that required for a CaMK-2–calmodulin interaction. However, at higher $[Ca^{2+}]$, the Rab3A-calmodulin association decreased relative to that of CaMK-2/calmodulin (Figs. 6 and 7). Moreover, the association of calmodulin to a particular β-granule protein would also depend on the relative abundance of β-granule Rab3A to other calmodulin-binding proteins present. This has been indicated in that overexpression of the constitutively active Rab3AQ1L variant in β-cells holds more of the β-granule calmodulin and inhibits Ca^{2+}-induced insulin exocytosis (14).

Collectively, the observations made in this study suggest a model in which at relatively low $[Ca^{2+}]_i$, a Rab3A-calmodulin interaction on a β-granule is favored. However, as $[Ca^{2+}]_i$ increases (as a result of opening of L-type Ca^{2+} channels [2]), there is a transfer of calmodulin to an alternative calmodulin-binding protein on β-granule that has a higher affinity for calmodulin at elevated $[Ca^{2+}]_i$, such as CaMK-2. This then results in activation of CaMK-2 in the vicinity of a β-granule, perhaps even at the site of exocytosis. Then, in an ensuing step, the activated CaMK-2 acts positively to phosphorylate an "exocytotic protein" and enhance either the transport of a β-granule to the plasma membrane and/or the mechanism of insulin exocytosis (4). Indeed, CaMK-2 has been implicated to play a role in the mechanism of regulated exocytosis (6), including insulin release from β-cells (4,46). Notwithstanding, it must be emphasized that CaMK-2 was only used as a model calmodulin-binding protein in these studies, and that a Ca^{2+}-dependent exchange of Rab3A-bound calmodulin to other calmodulin-binding proteins, such as calcineurin or myosin light-chain kinase (47), should not be ruled out. As such, it will be important to identify the appropriate calmodulin-binding β-granule protein that competes for Rab3A-bound calmodulin at higher $[Ca^{2+}]_i$. If this is indeed a Ca^{2+}/calmodulin-dependent protein kinase or phosphatase, then the substrates whose phosphorylation state can directly influence the mechanism-regulated insulin exocytosis will also need to be identified. Notwithstanding this, the biochemical characteristics of a Rab3A-calmodulin interaction in β-cells are consistent with a role in limiting the quantity of the exocytotic events in the β-cell and, as such, contributing to the overall control of insulin release (14).

ACKNOWLEDGMENTS

This work was supported by National Institutes of Health Grant DK-47919 and Pfizer.

We thank A.J. Lanzetti for access to a protein sequencer, Dr. P. De Camilli (Yale University) for MSS4 antisera, Dr. Ian Macara (University of Virginia) for the Rab3A variant constructs to generate recombinant protein, and Eli Lilly for [^{125}I]insulin.

REFERENCES

1. Prentki M: New insights into pancreatic β-cell metabolic signaling in insulin secretion. *Eur J Endocrinol* 134:272–286, 1996
2. Ashcroft FM, Proks P, Smith PA, Ammala C, Bokvist K, Rorsman P: Stimulus-secretion coupling in pancreatic beta cells. *J Cell Biochem* 55 (Suppl.):54–65, 1994
3. Deeney JT, Prentki M, Corkey BE: Metabolic control of β-cell function. *Semin Cell Dev Biol* 11:267–275, 2000
4. Easom RA: β-Granule transport and exocytosis. *Semin Cell Dev Biol* 11:253–266, 2000
5. Wollheim CB, Lang J, Regazzi R: The exocytotic process of insulin secretion and its regulation by Ca^{2+} and G-proteins. *Diabetes Rev* 4:276–297, 1996
6. Südhof TC: The synaptic vesicle cycle: a cascade of protein-protein interactions (Review). *Nature* 375:645–653, 1995
7. Rothman JE, Wieland FT: Protein sorting by transport vesicles. *Science* 272:227–234, 1996
8. Zerial M, Stenmark H: Rab GTPases in vesicular transport. *Curr Opin Cell Biol* 5:613–620, 1993
9. Geppert M, Bolshakov VY, Siegelbaum SA, Takei K, De Camilli P, Hammer RE, Südhof TC: The role of Rab3A in neurotransmitter release. *Nature* 369:493–497, 1994
10. Holz RW, Brondyk WH, Senter RA, Kuizon L, Macara IG: Evidence for the involvement of Rab3A in Ca^{2+}-dependent exocytosis from adrenal chromaffin cells. *J Biol Chem* 269:10229–10234, 1994
11. Geppert M, Goda Y, Stevens CF, Südhof TC: The small GTP-binding protein Rab3A regulates a late step in synaptic vesicle fusion. *Nature* 387:810–814, 1997
12. Senyshyn J, Balch WE, Holz RW: Synthetic peptides of the effector-binding domain of rab enhance secretion from digitonin-permeabilized chromaffin cells. *FEBS Lett* 31:41–46, 1992
13. Park JB, Farnsworth CC, Glomset JA: Ca^{2+}/calmodulin causes Rab3A to dissociate from synaptic membranes. *J Biol Chem* 272:20857–20865, 1997
14. Coppola T, Perret-Menoud V, Luthi S, Farnsworth CC, Glomset JA, Regazzi R: Disruption of Rab3-calmodulin interaction, but not other effector interactions, prevents Rab3 inhibition of exocytosis. *EMBO J* 18:5885–5891, 1999
15. Burton J, Roberts D, Montaldi M, Novick P, De Camilli P: A mammalian guanine-nucleotide releasing protein enhances function of yeast secretory protein Sec4. *Nature* 361:464–467, 1993
16. Burstein ES, Brondyk WH, Macara IG: Amino acid residues in the Ras-like GTPase Rab3A that specify sensitivity to factors that regulate the GTP/GDP cycling of Rab3A. *J Biol Chem* 267:22715–22718, 1992
17. Ostermeier C, Brunger AT: Structural basis of Rab effector specificity: crystal structure of the small G protein Rab3A complexed with the effector domain of Rabphilin-3A. *Cell* 96:363–374, 1999
18. Olszewski S, Deeney JT, Schuppin GT, Williams KP, Corkey BE, Rhodes CJ: Rab3A effector domain peptides induce insulin exocytosis via a specific interaction with a cytosolic protein doublet. *J Biol Chem* 269:27987–27991, 1994

19. Li G, Regazzi R, Balch WE, Wollheim CB: Stimulation of insulin release from permeabilized HIT-T15 cells by a synthetic peptide corresponding to the effector domain of the small GTP-binding protein Rab3. *FEBS Lett* 327:145–149, 1993
20. Chick WL, Warren S, Chute RN, Like AA, Lauris V, Kitchen KC: A transplantable insulinoma in the rat. *Proc Natl Acad Sci U S A* 74:628–632, 1977
21. Hutton JC: The insulin secretory granule. *Diabetologia* 32:271–281, 1989
22. Alarcón C, Lincoln B, Rhodes CJ: The biosynthesis of the subtilisin-related proprotein convertase PC3, but not that of the PC2 convertase, is regulated by glucose in parallel to proinsulin biosynthesis in rat pancreatic islets. *J Biol Chem* 268:4276–4280, 1993
23. Oberhauser AF, Monck JR, Balch WE, Fernandez JM: Exocytotic fusion is activated by Rab3a peptides. *Nature* 360:270–273, 1992
24. Padfield PJ, Balch WE, Jamieson JD: A synthetic peptide of Rab3a effector domain stimulates amylase release from permeabilized pancreatic acini. *Proc Natl Acad Sci U S A* 89:1656–1660, 1992
25. O'Neil KT, DeGrado WF: How calmodulin binds its targets: sequence independent recognition of amphiphilic alpha-helices. *Trends Biochem Sci* 15:59–64, 1990
26. Fernandez J, Andrews L, Mische SM: An improved procedure for enzymatic digestion of polyvinylidene difluoride–bound proteins for internal sequence analysis. *Anal Biochem* 218:112–117, 1994
27. Fernandez J, DeMott M, Atherton D, Mische SM: Internal protein sequence analysis: enzymatic digestion for less than 10 micrograms of protein bound to polyvinylidene difluoride or nitrocellulose membranes. *Anal Biochem* 201:255–264, 1992
28. Shirataki H, Takai Y: Purification and properties of Rabphilin-3A. *Methods Enzymol* 257:291–302, 1995
29. Tsien RY, Rink TJ: Neutral carrier ion-selective microelectrodes for measurement of intracellular free calcium. *Biochim Biophys Acta* 599: 623–638, 1980
30. Nojima H: Structural organization of multiple rat calmodulin genes. *J Mol Biol* 208:269–282, 1989
31. Potter S, DeMott M, Aswad DW: In vitro aging of calmodulin generates isoaspartate at multiple Asn-Gly and Asp-Gly sites in calcium-binding domains II, III, and IV. *Prot Sci* 2:1648–1663, 1993
32. Crivici A, Ikura M: Molecular and structural basis of target recognition by calmodulin. *Ann Rev Biophys Biomol Struct* 24:85–116, 1995
33. Braun AP, Schulman H: The multifunctional calcium/calmodulin dependent protein kinase: from form to function. *Ann Rev Physiol* 57:417–445, 1995
34. Bronstein JM, Farber DB, Wasterlain CG: Regulation of type-II calmodulin kinase: functional implications. *Brain Res Brain Res Rev* 18:135–147, 1993
35. Zahraoui A, Touchot N, Chardin P, Tavitian A: The human Rab genes encode a family of GTP-binding proteins related to yeast YPT1 and SEC4 products involved in secretion. *J Biol Chem* 264:12394–12401, 1989
36. Vallar L, Biden TJ, Wollheim CB: Guanine nucleotides induce Ca^{2+}-independent insulin secretion from permeabilized RINm5F cells. *J Biol Chem* 262:5049–5056, 1987
37. Regazzi R, Ravazzola M, Lezzi M, Lang JC, Zahraoui A, Andereggen E, Morel P, Takai Y, Wollheim CB: Expression, localization and functional role of small GTPases of the Rab3 family in insulin secreting cells. *J Cell Sci* 109:2265–2273, 1996
38. Fischer von Mollard G, Stahl B, Li C, Südhof TC, Jahn R: Rab proteins in exocytosis. *Trends Biochem Sci* 19:164–168, 1994
39. Edwardson JM, An S, Jahn R: The secretory granule protein syncollin binds to syntaxin in a Ca^{2+}-sensitive manner. *Cell* 90:325–333, 1997
40. Ann K, Kowalchyk JA, Loyet KM, Martin TF: Novel Ca^{2+}-binding protein (CAPS) related to UNC-31 required for Ca^{2+}-activated exocytosis. *J Biol Chem* 272:19637–19640, 1997
41. Lin RC, Scheller RH: Mechanisms of synaptic vesicle exocytosis. *Annu Rev Cell Dev Biol* 16:19–49, 2000
42. Li C, Ullrich B, Zhang JZ, Anderson RG, Brose N, Südhof TC: Ca^{2+}-dependent and -independent activities of neural and non-neural synaptotagmins. *Nature* 375:594–599, 1995
43. Littleton JT, Bai J, Vyas B, Desai R, Baltus AE, Garment MB, Carlson SD, Ganetzky B, Chapman ER: Synaptotagmin mutants reveal essential functions for the C2B domain in Ca^{2+}-triggered fusion and recycling of synaptic vesicles in vivo. *J Neurosci* 21:1421–1433, 2001
44. Wollheim CB, Pozzan T: Correlation between cytosolic free Ca^{2+} and insulin release in an insulin secreting cell line. *J Biol Chem* 259:2262–2267, 1984
45. Bokvist K, Eliasson L, Ammala C, Renstrom E, Rorsman P: Co-localization of L-type Ca^{2+} channels and insulin-containing secretory granules and its significance for the initiation of exocytosis in mouse pancreatic B-cells. *EMBO J* 14:50–57, 1995
46. Easom RA: CaM kinase II: a protein kinase with extraordinary talents germane to insulin exocytosis. *Diabetes* 48:675–684, 1999
47. Molina JM, Cooper GJ, Leighton B, Olefsky JM: Induction of insulin resistance in vivo by amylin and calcitonin gene-related peptide. *Diabetes* 39:260–265, 1990